THE STANDARD MODEL 30 YEARS OF GLORY

Jacques Lefrançois
Laboratoire de l'Accélérateur Linéaire
IN2P3-CNRS et Université PARIS-SUD
Centre Scientifique d'Orsay - Bât. 200 - B.P. 34
91898 ORSAY Cedex (France)
lefranco@lal.in2p3.fr

In these three lectures, I will try to give a flavour of the achievements of the past 30 years, which saw the birth, and the detailed confirmation of the Standard Model (SM). However I have to start with three disclaimers:

- Most of the subject is now history, but I am not an historian, I hope the main core will be exact but I may err on some details.
- Being an experimentalist, I will mostly focus on the main experimental results, giving, when appropriate, some emphasis to the role of well conceived apparatus. This does not mean that I minimise the key role of theorist, it only reflects the fact that the same story told by a theorist would correspond to another interesting series of lectures.
- Finally, in some cases, I may show a bias coming from the fact that I have seen from closer what has happened in Europe.

The three lectures will cover:
QCD from the discovery of deep inelastic scattering at SLAC to the gluon discovery at Petra.
Weak interaction and the quarks and leptons families, from the neutral current discovery to the members of the third family.
Finally, I will spend some time on LEP and SLC results since they are (or have been) ideal machines for detailed standard model studies, however since these last results are well covered in many schools and conferences it has been greatly shortened in the written version.

1. QCD

1.1. DEEP INELASTIC AT SLAC

Up to the 1967 SLAC discovery, electron scattering was used to measure elastic and inelastic nuclear and nucleon form factors. In the language of the time the nucleon form factors (which revealed the charge distribution inside the nucleon) corresponded to the probability of hitting the meson cloud around the nucleon and keeping the nucleon intact or transforming it into an excited state (N*). In modern language they represent the probability to hit a quark inside the nucleon and nevertheless keeping the nucleon intact or transforming it into an excited 3 quark state.

The experimental breakthrough in 1967 was the construction of a high intensity 20 GeV electron linear accelerator. The apparatus was a spectrometer rather classical (for linac apparatus). The accent was put on reliability and very powerful online computer control (which was new for the time). The first result in 1968 (fig.1) showed clearly that something new was happening and that the Q^2 dependence of the cross-section was quite different from previous elastic and inelastic results and similar to what would be expected to result of scattering on point-like objects.

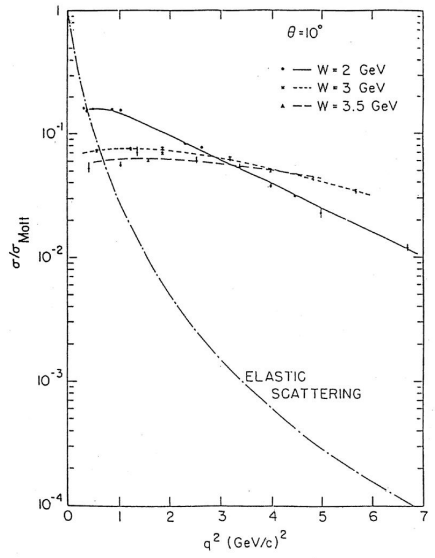

Figure 1 The elastic and inelastic cross-section as function of Q^2 showing the absence of form factor at large excitation energy.

The main variables are defined below:

$$Q^2 = 2EE'(1 - cos\theta) = 4EE'sin^2\theta/2$$

$$\nu = E - E' \quad \omega = \frac{2M\nu}{Q^2} \quad x = \frac{Q^2}{2M\nu}$$

and the cross-section, in the most general case is

$$\frac{d^2\sigma}{d\Omega dE'} = \sigma_{Mott}(W_2 + 2W_1 tg^2\theta/2)$$

where $\sigma_{M_{ott}}$ is a point-like cross-section.

In 1969 Bjorken predicted scaling of the W structure functions i.e. that, as Q^2 and ν went to large values 2MW1(ν,Q) and νW2(ν,Q) would become only functions of the scaling variable ω or x. Scaling was experimentally confirmed as shown in figure 2.

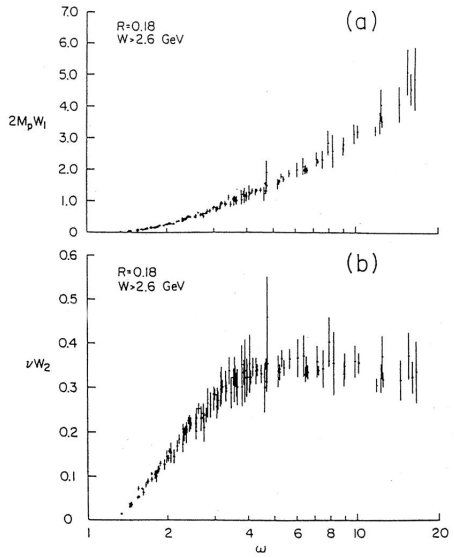

Figure 2 Structure functions at various Q^2 as function of w, showing scaling behaviour.

Actually, already in 1966, using current algebra and sum rules Bjorken had derived the following formula

$$\lim_{E\to\infty}\left[\frac{d\sigma}{dQ^2}ep + \frac{d\sigma}{dQ^2}en\right] \geq \frac{2\pi\alpha^2}{Q^4}$$

This implied clearly a cross-section varying with Q^2 in the way expected in the case of scattering from point-like objects.

However it went unnoticed by the experimentalist preparing the SLAC experiment and the result shown in figure 1 came as a surprise.

More generally the theoretical framework was badly understood by experimentalists until about 1969. In that year Feynman invented his very intuitive parton model to explain the deep inelastic results. The parton were point-like constituents inside the nucleon; in the frame where the nucleon momentum is very large, the collision is instantaneous and the partons are independent. If the nucleon has a momentum P the partons have momentum xP. The kinematics and dynamics is then a very simple electron parton elastic scattering and the following formula is derived

$$\nu W_2(\nu, Q^2) = F_2(x) = \sum_1^N Q_i^2 \times f_i(x)$$

$f_i(x)$ being the probability of finding a parton carrying a fraction x of the momentum and the total probability being a sum over all partons weighted by the square of their charges. The nature of these partons was not immediately obvious but clear candidates were the u and d type quarks invented earlier by Gell-Man as constituents of the nucleon.

In the quark model therefore:

$$F_2^p(x) = x\left[Q_u^2(u_p(x) + \bar{u}_p(x)) + Q_d^2(d_p(x) + \bar{d}_p(x))\right]$$

If the quarks are the only particles carrying a fraction of a deuteron (or other I = 0 nuclei) momentum, then integration of the momentum distribution should give 1, and the integral of the structure function should give the quark charge:

$$\left(Q_u^2 + Q_d^2\right)/2 = 5/18 = .28$$

In case of the 2/3, 1/3 charge assignment the integral should be 0.28. Experimentally a value of 0.14 $\pm$ 0.005 was found: either the quark interpretation of partons was wrong or something else (chargeless) was carrying 50% of the nucleon momentum. (We of course now know that it is the gluons). Another information was needed to solve this riddle, it was provided by neutrino experiments.

1.2. NEUTRINO SCATTERING RESULTS (1972-1974)

In this case the experimental breakthrough was the existence of a high intensity neutrino beam at the CERN 28 GeV PS and the construction of a large heavy liquid bubble chamber Gargamelle.

The neutrino beam was made possible by the invention around 1966 by Simon Van der Meer of the neutrino horn which was used to focus pions over a wide momentum and angular band. The decay of the pions giving rise to the neutrino beam. The improvement of an order of magnitude in neutrino flux can be seen in figure 3.

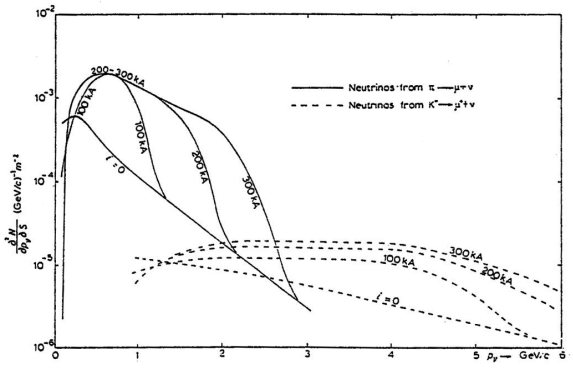

Figure 3 The neutrino yield, as function of energy for various values of the horn current.

The decision of constructing Gargamelle (fig. 4) was an extremely effective one for doing medium energy neutrino physics.

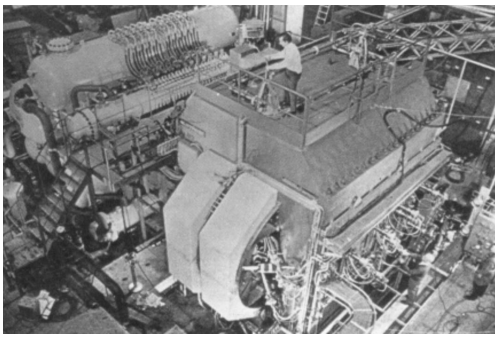

Figure 4 The Gargamelle bubble chamber.

Gargamelle dimensions were 4.5 m in length and 1.5 m in diameter; it could be filled with freon of density 1.2 to 1.5 a clear mass advantage compared to liquid hydrogen bubble chambers. The short radiation and interaction length of freon together with the bubble chamber resolution

meant that neutrino reactions could be followed in detail which was a decisive advantage for few GeV neutrino physics when compared to massive sampling calorimeter instruments which will be more suited for high energy experiments.

Finally warm liquid and a warm coil magnet meant a simpler and faster construction compared to that of the future liquid hydrogen bubble chambers built later at Fermilab and CERN.

At the 1972 Rochester conference, results were presented on 1000 neutrino and 1000 antineutrino interactions of energy larger than 1 GeV, by the Gargamelle collaboration.

In the case of ν and $\bar{\nu}$ interactions, the cross-section distinguishes between quarks and antiquarks and are given by the following formulas, where X_1 an X_2 are the fraction of the incident particles momenta carried by the interacting quarks:

$$\frac{d^2\sigma^{\nu,\bar{\nu}}}{dxdy} = \frac{G^2ME}{\pi}\left[(1-y)F_2(x) + \frac{y^2}{2}\times 2xF_1(x) \pm y\left(1-\frac{y}{2}\right)xF_3\right]$$

$$2xF_1 \approx F_2$$

$$\sigma_\nu + \sigma_{\bar{\nu}} = \frac{G^2ME}{\pi}\frac{4}{3}\int_0^1 F_2 dx$$

$$\int_0^1 F_2 dx = \int x\left[u + \bar{u} + d + \bar{d}\,\right]dx = 0.47 \pm 0.07$$

Results confirmed that 50% of the nucleon's momentum is transported by particles without charge and therefore without electromagnetic and weak interactions (the gluons). Comparison between electron nucleon and neutrino nucleon interactions confirmed the fractional charge of quarks.

Furthermore from the difference $\nu - \bar{\nu}$ the xF_3 function was obtained; and it could be shown that valence quarks dominate the momentum distribution:

$$B = \frac{\int_0^1 xF_3}{\int_0^1 F_2} = \frac{\int u + d - \bar{u} - \bar{d}}{\int u + d + \bar{u} + \bar{d}} = 0.9 \pm .1$$

also the integral over F_3 gives the number of valence quarks. At the 1974 Rochester conference Gargamelle announced :$\int_0^1 F_3 = 3.2 \pm .6$ a striking confirmation of the standard model.

By 1973 the QCD theory had been proposed and strong interaction was finally understood as a force between coloured quarks mediated by an octet of coloured gluons. As a consequence of the theory a certain

number of phenomena could be predicted and calculated in perturbation theory.

1.3. $\mathbf{R(e^+e^-)}$

The prediction of a modification of $\mathrm{R}(e^+e^-)$ was one of the earliest predicted consequences of the colour concept.

If the production of hadrons in e^+e^- annihilation at high energy is considered to result from the creation of quark antiquark pairs the predicted ratio of the parton production cross-section to the μ pair cross-section will be higher by a factor 3 because of the 3 colour possibilities.

$$R = \frac{\sigma_{had}}{\sigma_{\mu^+\mu^-}} = 3 \times \sum_1^{n_f} Q_i^2 + n_{\ell \neq e,\mu}$$

The first term is the contribution of $q\bar{q}$ pairs and the second one is the contribution of a new lepton family (of charge one and without colour factor) which has to be added since it was at that time indistinguishable from hadronic events. The first results in 1973 were obtained at 4-5 GeV at the CEA storage ring (built by Harvard-MIT). They were inconclusive because of the ignorance of the charmed quark and τ lepton existence (the τ pairs were observed as hadrons since essentially everything not identified as Bhabba events or μ pair events were called hadrons). As a result the cross-section was observed to be higher than prediction (fig. 5).

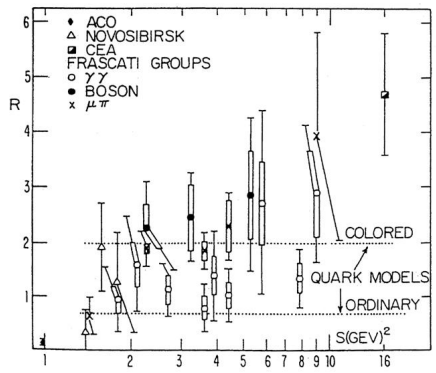

Figure 5 The R value as function of s, the square of the center of mass energy.

Even in 1975 after the discovery of the c quark the SLAC MARKI results (fig. 6) were thought to be in disagreement with predictions.

The observed R value at high energy was about 5.0 while the predicted value was 3.33. This fact was one of the reasons of the slow acceptance of QCD. It took the confirmation of the τ lepton existence in 1975-1977 and the calculation of the first order QCD correction $(1. + \alpha s/\pi)$ to change gradually the predicted value to about 4.6.

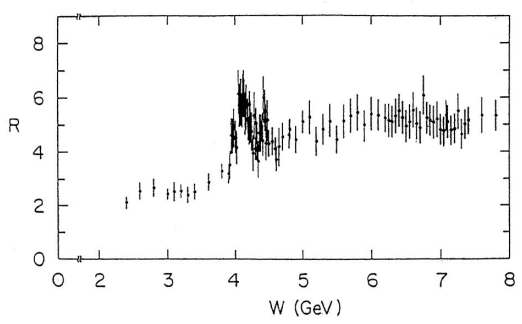

Figure 6 R values obtained by MARKI as function of the center of mass energy.

1.4. SCALING VIOLATION

By analogy with QED, QCD radiative corrections were expected in deep inelastic cross-section of electrons muons or neutrinos (fig.7).

As a result, the parton structure functions were predicted to become Q^2 dependent. There were some early but inconclusive sign of this phenomenon in 1972 SLAC data but which could not be disentangled from threshold effects at low Q^2. By the 1975 lepton photon conference evidence of scaling violation were presented from the SLAC experiment (fig. 8) and from a FERMILAB experiment on muon iron scattering at high energy done by the Cornell-Michigan state-Berkeley-La Jolla collaboration (fig. 9).

For a quantitative use of scaling violation to extract $\alpha_s(Q^2)$, it was necessary to wait for theoretical and experimental progress (after 1977).

By 1977 the DGLAP equations were invented which gave a quantitative prescription of structure function evolution.

For increasing Q^2 the valence quark structure function is depleted by gluon emission feeding in the gluon structure function whose evolution in turn modifies the sea quark structure functions. Because of the ignorance of the gluon structure function, the evolution studies used to extract accurate values of α_s had to be restricted to the valence quark structure function obtained either by neutrino interaction, or by restricting the analyses to high x values where sea quark effects are negligible.

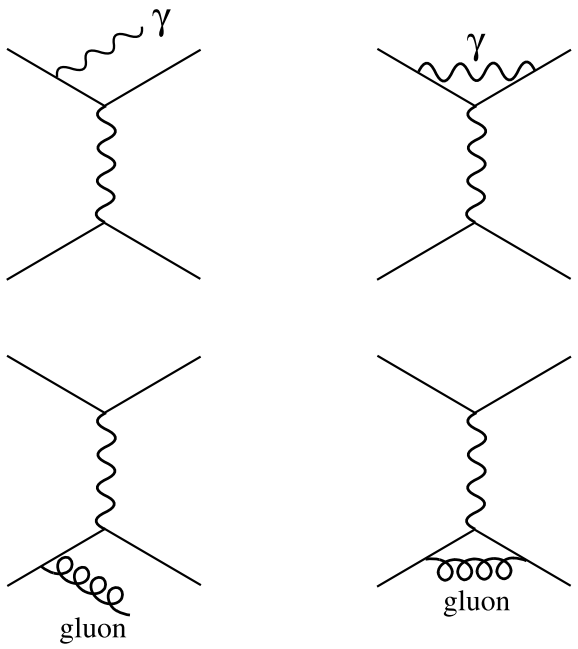

Figure 7 QED and QCD radiative corrections to deep inelastic cross-section.

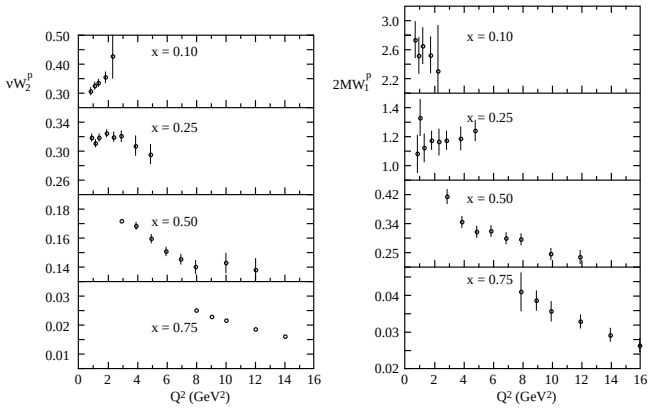

Figure 8 SLAC results on Q^2 variation of structure functions.

Both methods required a large number of interactions, which delayed the obtention of accurate values. An example of such an analysis (done in 1992) giving $\alpha_s(Mz) = 0.111 \pm 0.003$ is shown on figure 10.

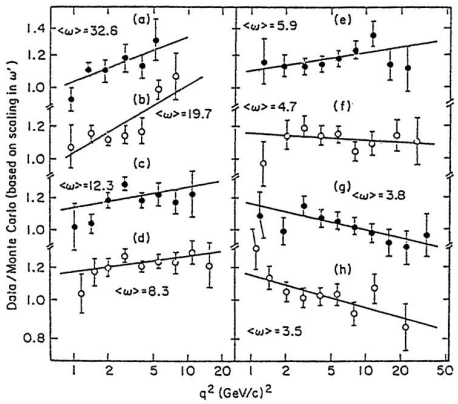

Figure 9 Result of the CMBL experiment at Fermilab showing Q^2 variation of structure functions.

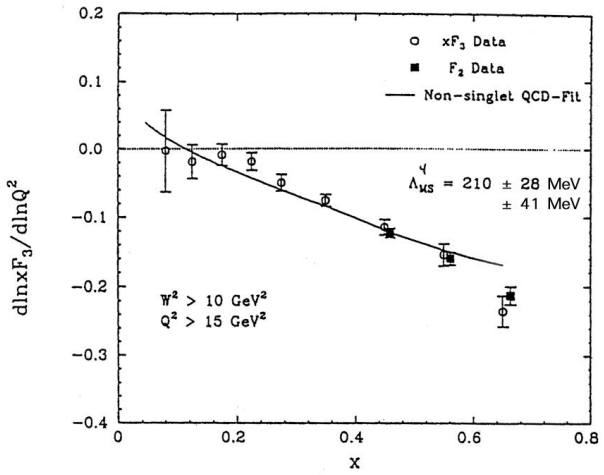

Figure 10 Extraction of Λ_{QCD} from the shape of the valence quark structure function of high x values by the CCFR neutrino experiment at Fermilab.

Theoretical corrections, from higher order QCD diagrams, and from $1/Q^2$ threshold effects had also to be taken into account. By 1999 with the inclusion of next to next to leading order corrections and high accuracy data, results converged to $\alpha_s(Mz) = 0.1172 \pm 0.0045$ which as we will see later is in good agreement with LEP and SLC results.

1.5. DRELL-YAN REACTIONS

After the discovery of deep inelastic scattering, it was rapidly realised that there should exist a corresponding effect in hadron collisions where quark and antiquark would annihilate to create μ or electron pairs: the so called Drell-Yan effect (1970) (Fig. 11).

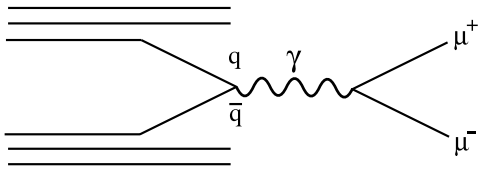

Figure 11 Feynman diagram of the Drell-Yan effect.

Application of QCD meant that the predicted cross-section was smaller by a factor 3 taking into account that annihilation can only happen if the colour of the quark and antiquark match each other. As in deep inelastic scattering, the transverse momentum of the partons are neglected in first order, kinematics and cross-section are then described by the following formulas, where X_1 and X_2 are the fraction of the incident particles momenta carried by the interacting quarks:

$$M^2_{\mu\mu} = X_1 X_2 s$$

$$X_{\mu\mu} = \frac{2P*_L}{\sqrt{s}} = X_1 - X_2$$

$$\frac{d^2\sigma}{dX_1 dX_2} = \frac{4\pi\alpha^2}{3sX_1X_2} \times \frac{1}{3} \times \sum_i \frac{Q_i^2}{X_1X_2} \left[f_i^{h1}(X_1) f_{\bar{i}}^{h2}(X_2) + f_{\bar{i}}^{h1}(X_1) f_i^{h2}(X_2) \right]$$

The first experiment was done, in 1970, by Lederman et al., at Brookhaven, with a 28 GeV proton beam interacting on an iron target and producing muon pairs. Hadrons were filtered by an iron beam dump and the muon energies measured by range. Because of the crude energy measurement and angle smearing from multiple scattering in the beam dump, the mass resolution was very coarse ($> 15\%$). Because of this the results were impossible to interpret and even at the 1974 Rochester conference in London the rapporteur presenting the results (Fig. 12) concluded:"it is fairly clear that theory doesn't have much to say in regard to the cross-section measured in this experiment".
Of course we now know that the huge discrepancy was due to the production of the J/ψ resonance followed by its decay in muon pair.

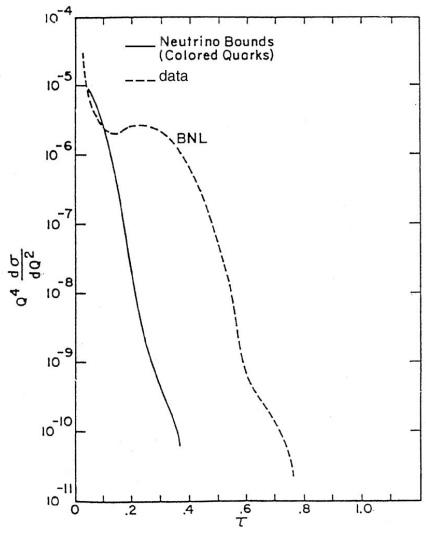

Figure 12 The first Drell-Yan cross-section measured at BNL by Lederman et al. as function of the reduced mass $\tau = M/\sqrt{s}$.

The experimental situation started to improve around 1977 when the CFS collaboration at Fermilab did a more accurate experiment both because of the higher beam energy and because of the much better apparatus (fig. 13) which will be described when the upsilon discovery will be discussed.

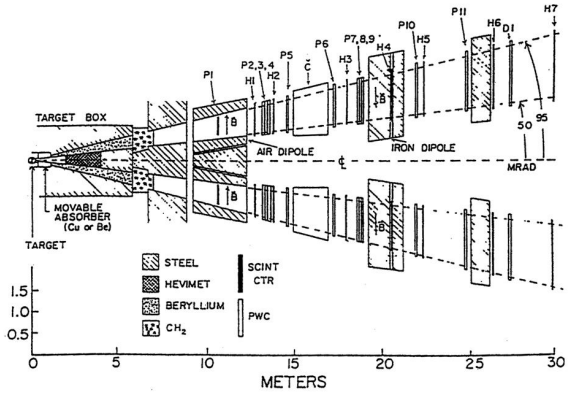

Figure 13 The two arm spectrometer used to measure Drell-Yan cross-section at Fermilab.

By the 1978 Rochester conference in Tokyo good results were presented by the CFS collaboration (and by 3 ISR experiments with smaller number of events). The results (Fig. 14) seemed to be in agreement with the Drell-Yan prediction, however the prediction depended on the antiquark structure function extracted from neutrino scattering data with rather large statistical and systematical errors.

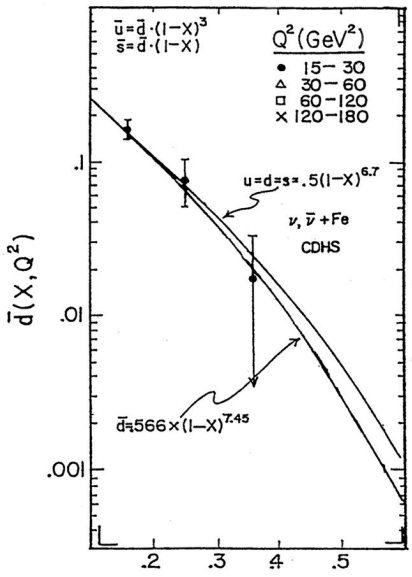

Figure 14 Nucleon six quark structure function extracted from Drell-Yan cross-section (data points) compared to fit of neutrino results.

However by 1979 it was realised that the tree level prediction of Drell-Yan cross-section should receive large QCD correction; it was the so-called K factor calculation. The basis of the argument is that when the vertex correction of QCD are calculated at negative Q^2 (deep inelastic) or positive Q^2 (Drell-Yan) the correction differ by an extra factor of $(\ln(-1))^2$ or π^2, in the case of Drell-Yan. The final first order Drell-Yan QCD correction was therefore of order 0.6 and it was conjectured that the series $1 + 0.6$ calculated to higher order could be exponentiated and result in a K factor correction of $\exp(0.6)=1.8$ to the predicted cross-section.

Results on proton proton and pion proton cross-section gave, in 1979, early indication of the presence of the K factor; however the clearest result was presented in 1980 by measurements, by the NA3 collaboration at CERN, of antiproton (and proton) Drell-Yan cross-section on nuclei. The subtracted $(\bar{p} - p)$ N cross-section corresponds to pure valence quark interaction and can therefore be predicted accurately. As shown in figure 15 the measured and predicted structure functions agree very well; the measured K factor is 2.3 ± 0.4 in good agreement with the large predicted QCD correction.

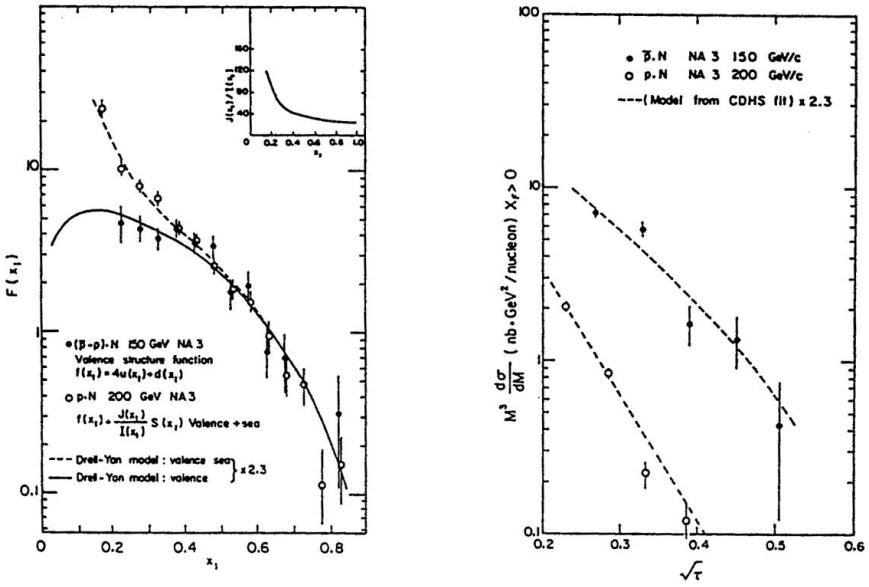

Figure 15 NA3 results on $\bar{P}N$ and PN Drell-Yan measurements compared to fit of nucleon valence quark cross-section.

1.6. OBSERVATION OF JETS

Almost immediately after the interpretation of deep inelastic scattering as lepton quark collisions, the question of the fate of the recoiling quark was raised. Already, in the 1970-1972 period, it was predicted that this recoiling quark would give birth to a jet by some sort of outside inside cascade creating $q\bar{q}$ pairs and then mesons (fig. 16).

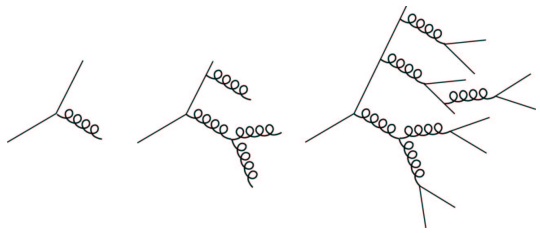

Figure 16 Parton shower cascade.

Gradually there was a better modelling of the jet as a parton shower cascade ending up in a hadronisation stage where small virtuality quark antiquark pairs recombine to form mesons of various spin assignment. The theoretical breakthrough happened in 1984 with the introduction of angular ordering in the parton shower (i.e. later partons in the parton shower are emitted at smaller angles). To prove experimentally the existence of jets, high collision energy were needed such that the hadronisation transverse momentum (of order 0.3 GeV/c per particle) would be much smaller than the longitudinal momentum of each of the jet particles.

The first evidence came in 1975 from the MARKI experiment studying 6-7 GeV e^+e^- collisions at the SPEAR/SLAC machine. The analysis consisted in, first defining an axis which minimised the p_t of particles (the Thrust axis), then the sphericity (S) with respect to this axis is defined as

$$S = \frac{3\sum P_{Ti}^2}{2\sum \vec{p}_i^2}$$

Clearly S = 0 corresponds to an infinitely narrow jet and S = 1 to an isotropic event. Contrary to what was expected for a phase space model of particle production, it was found that the mean sphericity decreased with collision energy (fig. 17) as expected in a jet model.

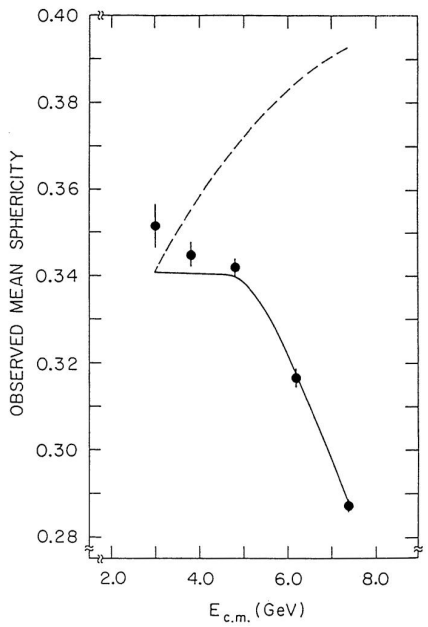

Figure 17 Mean sphericity as function of center of mass energy.

And at high energy, the S distribution of events was characteristics of a jet model (fig. 18).

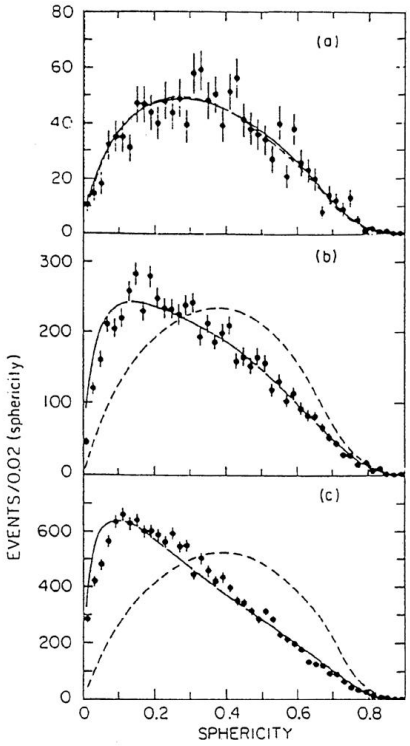

Figure 18 Event distribution as function of sphericity value for 3 center of mass energy. (a) at 3 GeV, (b) at 6 GeV, (c) at 7.4 GeV. The dashed line is a phase space model prediction, while the full line represents the jet model prediction.

One bonus of the jet observations was obtained with polarised e^+e^- beams. It had been predicted by Sokolov and Ternov, and observed before 1970 that in storage rings e^+ and e^- get gradually polarised by the emission of synchrotron radiation (except at some energies where depolarisation resonances exist in the machine). The beam polarisation P affects the azimuthal angular distribution of the annihilation product

$$e^+e^- \to \mu^+\mu^- \to 1 + cos^2\theta + P^2 sin^2\theta cos2\varphi$$

If quark have spin 1/2, a similar formula was expected:

$$e^+e^- \to q\bar{q} \to 1 + cos^2\theta + P^2\alpha sin^2\theta cos2\varphi$$

where θ and ϕ of the quarks is identified to θ and ϕ of the thrust axis. P was obtained from $\mu\mu$ events $P^2 = 0.47 \pm 0.05$

$$\alpha = \frac{\sigma_T - \sigma_L}{\sigma_T + \sigma_L}$$

Since the ϕ acceptance is very uniform systematical effects were negligible, while the observation of the quark spin through the polar angle distribution would have been much more delicate.

The results obtained (fig. 19) were a clear confirmation of the spin of the produced partons and a proof of the usefulness of the jet concept.

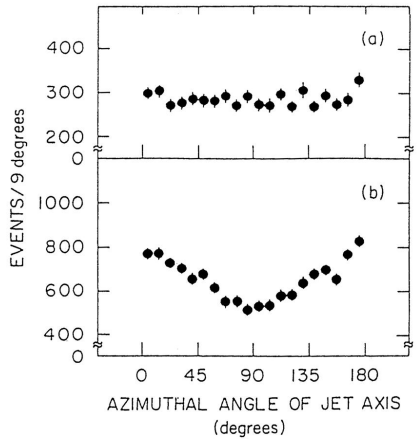

Figure 19 Jet angle orientation as function of azimuthal angle a) at 6.2 GeV where the beam polarisation is 0. b) at 7.4 GeV where beam polarisation exists.

Jets in hadronic collisions where much harder to observe. One expected a Pt distribution given by $\frac{d\sigma}{dp_t^2} \propto \frac{1}{P_t^4}$ in analogy with $\frac{d\sigma}{dQ^2} \propto \frac{1}{Q^4}$. However in almost all experiments a trigger was performed on a single high P_t particle which biased completely the jet observation. For the single particle a $\frac{1}{p_t^8}$ was observed which resulted from a complicated mixture of parton collision dynamics and parton fragmentation to a single particle. Even in 1980, (after 3 jet events had been observed in e^+e^- collisions at PETRA !), there existed no convincing and unbiased observation of jets in hadronic collisions. Either the energy was to low for isotropic experiments (NA5 experiment at the CERN SPS and similar experiments at FERMILAB) or apparatus were not isotropic enough (ISR).

The experimental breakthrough was obtained at the start of the CERN $p\bar{p}$ collider ($\sqrt{s} = 600$ GeV). At the 1982 Rochester conference in Paris, the UA2 experiment showed very convincing results. As we will see later the UA2 apparatus design was not as good as the UA1 to observe the W boson, but it was built in an almost ideal way to observe jets (fig. 20,21).

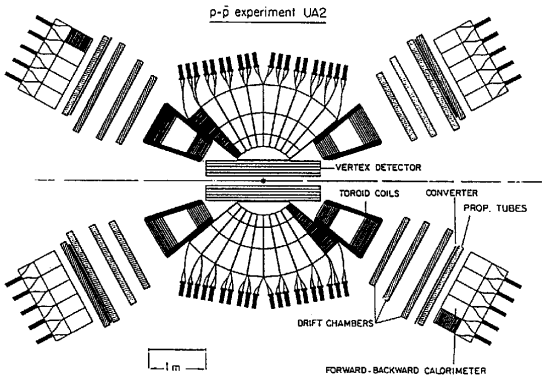

Figure 20 Polar view of the UA2 apparatus.

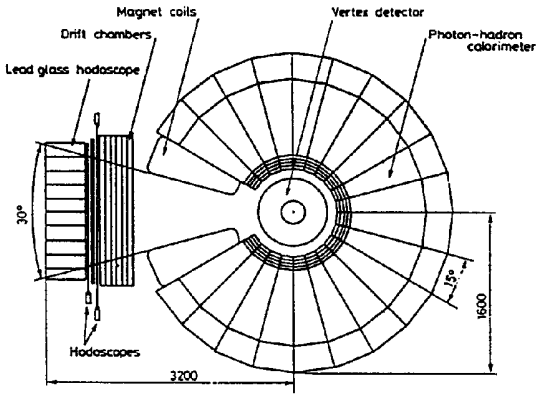

Figure 21 Azimuthal view of the UA2 apparatus.

It consisted essentially in cells of electromagnetic and hadronic calorimeter. The granularity was small for the time, 260 cells, (of $\Delta\theta \times \Delta\phi = 10^\circ \times 15^\circ$) even if it seems large compared to modern calorimeter. The trigger was an unbiased one looking for high E_t summed over all cells. It was immediately found that most of the E_t was concentrated in clusters of typically 5 cells (Fig. 22).

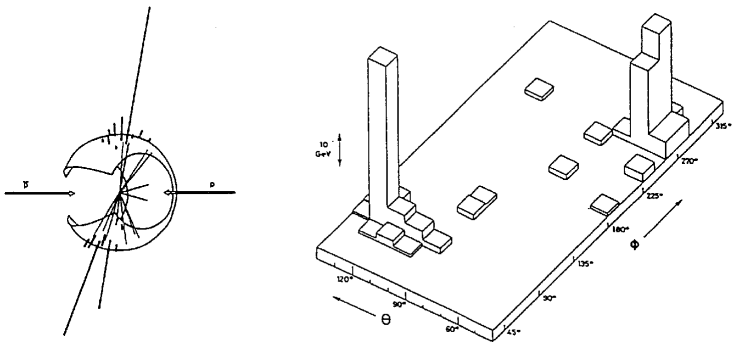

Figure 22 Angular distribution of energy in an event with $\sum E_t = 150$ GeV.

At $E_t > 80$ GeV close to 80% of the E_t was found in 2 clusters (Fig. 23).

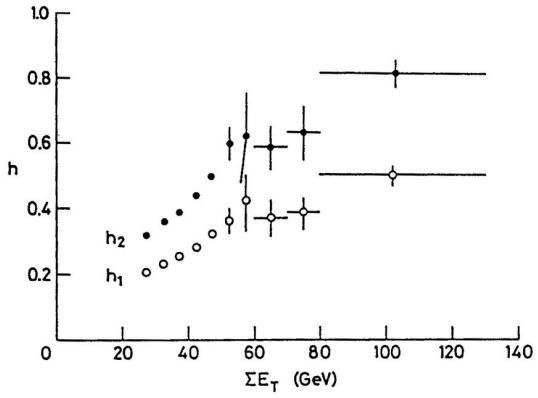

Figure 23 Fraction of the transverse energy of events measured in one (opened circles) or two jets (filled circles).

1.7. GLUON JET OBSERVATION

The idea that gluon bremsstrahlung existed, in analogy to photon radiation from charged particles, dates from the invention of QCD.

In 1976 there was a remarkable phenomenological paper by J. Ellis, M.K. Gaillard and G. Ross which pointed out that gluon radiation, in

e^+e^- hadronic collisions, would cause some 2-jet events to be "fat" on one side (contrary to pair creation of new particles which was expected to lead to events with two "fat" jets) and it was pointed out that eventually 3 jet events would occur. (Fig. 24).

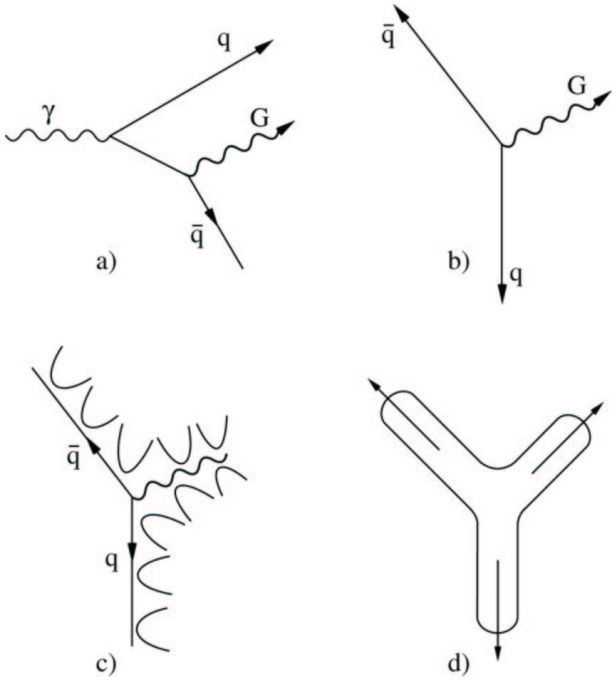

Figure 24 Schematics of gluon radiation as explained in the Ellis Gaillard Ross article.

Nevertheless the energy had to be high enough and the necessary analysis tools had to be developed by the experimentalist.

The Petra machine reached the necessary energies (27 GeV) in 1979. On the analysis side the idea was to choose, for each event, a plane which minimised the event transverse momentum perpendicular to this plane (Pt-out). At the 1979 June EPS meeting in Geneva Tasso showed a few of such planar events which possessed 3-jets structure (fig. 25) together with strikingly different Pt-in and Pt-out distributions. By the time of the electron-photon conference in Fermilab in August 1979 all four Petra experiments showed convincing distributions and the evidence for the gluon discovery was accepted.

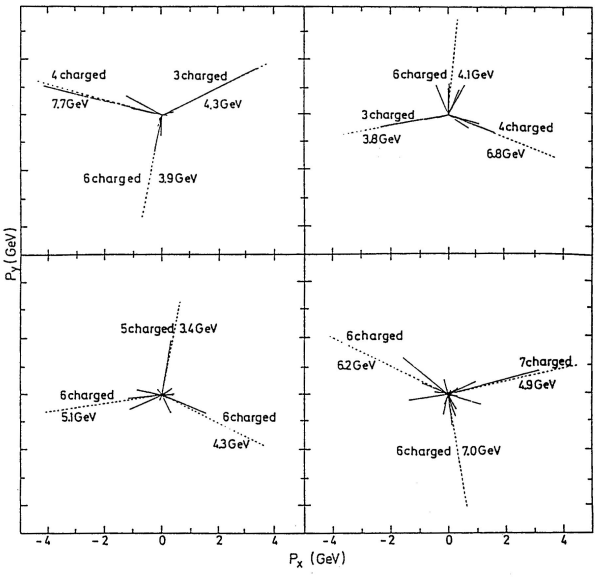

Figure 25 From candidates 3 jet events seen by Tasso in 1979.

2. WEAK INTERACTION AND QUARK AND LEPTON FAMILIES

2.1. NEUTRAL CURRENT DISCOVERY (1973-1974)

The discovery of neutral current by the Gargamelle experiment was one of the key discovery of the past 30 years. It allowed to confirm that the Glashow Salam Weinberg model was the correct electroweak theory. At that time, in the early seventies, other alternatives were proposed to deal with the diverging high energy behavior of the Fermi pointlike weak interaction, (for example the existence of heavy leptons or of diagonal currents).

Since the late 50's it was generally assumed (for example by Schwinger in 1957)that the pointlike nature of weak interaction was the result of the exchange of a very heavy charged particle ($W^{\pm}$), in contrast with the long-ranged QED force caused by the exchange of a massless photon.

In the late sixties the Glashow Salam Weinberg model was presented, it predicted the existence of a neutral partner of the $W^{\pm}$, the Z^0 particle and hence the existence of neutral current weak interactions.

A big stumbling block for this model, was the experimental absence of $\Delta S = 1$ neutral currents i.e. the absence or very small rates of decays like $K_L^0 \to \mu^+\mu^-$ or $K \to \pi\nu\bar{\nu}$. The Glashow, Iliopoulos, Maiani mechanism (GIM), invented in 1970, explained this puzzling fact by the predicted existence of a new quark the charm quark. Then in 1971 Veltman and t'Hooft proved that the electroweak theory was renormalizabled and showed higher order calculations could be performed.

Experimentally neutral currents were predicted to be seen in two types of neutrino interactions:

of leptonic type:

$$\bar{\nu}_\mu e^- \Rightarrow \bar{\nu}_\mu e^-$$

or

$$\nu_\mu e^- \Rightarrow \nu_\mu e^-$$

with background

$$\nu_e n \to e^- p$$
$$\bar{\nu}_e p \to e^+ + n$$
$$\hookrightarrow +\gamma \to e^+ e^-$$

or of hadronic type

$$\nu_\mu + N \Rightarrow \nu_\mu + X$$

with background

$$n + N \Rightarrow n + X$$

The background for the leptonic reaction was the elastic interaction on nucleons of the ν_e or $\bar{\nu}_e$ always present as a contamination in a ν_μ or $\bar{\nu}_\mu$ beam, the background from $\bar{\nu}_e$ being of course much smaller.

The background in the hadronic reaction was neutron scattering, the neutrons being produced by neutrino interaction at the end of the ν beam shielding.

As explained in the previous chapter, the Gargamelle bubble chamber started to take data in 1971. The fiducial mass was 4.5 tons out of a total mass of 20 tons. Gargamelle was an almost ideal apparatus for few GeV neutrino physics, it showed full details of the interaction and the reinteractions of neutrals. It was big enough (about 6 interaction length) to see attenuation of the incident neutron background, similarly muons could be identified by their absence of reinteraction in the liquid.

The first sign of neutral current was a $\bar{\nu}_\mu e^-$ scattering event observed in December 1972 (fig. 26). For the total exposure of 1.4×10^6 pictures 5 to 30 events were expected depending on the $\sin^2 \vartheta_{\mathrm{w}}$ value, finally 3 events were seen.

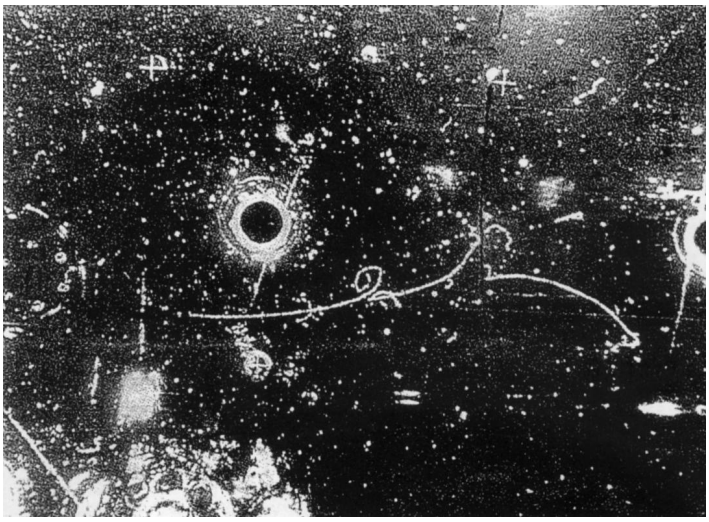

Figure 26 The first elastic $\bar{\nu}_\mu e^-$ scattering event seen in Gargamelle.

The big difficulty for the observation of hadronic neutral current events was the neutron background evaluation. As shown in figure 27 the neutron path length in the Gargamelle liquid was calibrated by looking at neutron reinteraction downstream from a neutrino interaction (the so called Associated Star).

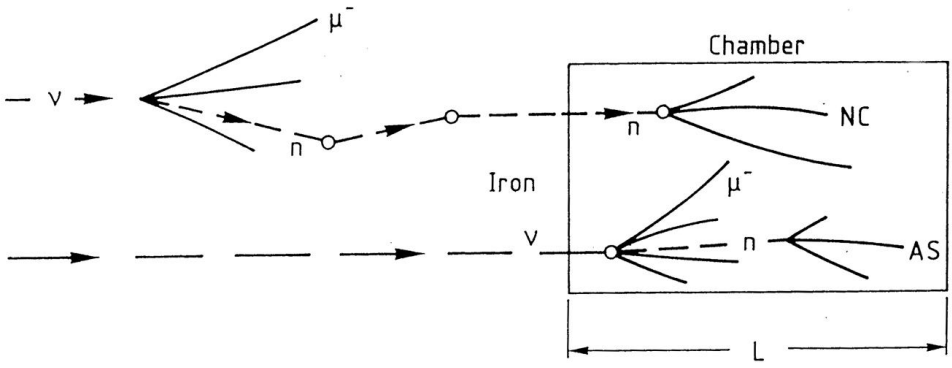

Figure 27 Schematics of neutron background events in Gargamelle and their probability and path length determination by associated stars (AS).

Knowing this path length one could predict the Z dependence of the neutron background events, while of course neutrino neutral current events were expected to be produced equally at all Z values. From the observed distribution (fig. 28), it was estimated that only 10 % of the muonless neutral current candidates were from neutron. From R the relative rate of the neutral current events to charge current events in ν_μ and $\bar{\nu}_\mu$ beam a value of $\sin^2\theta_w$ was extracted, the results are shown on figure 29.

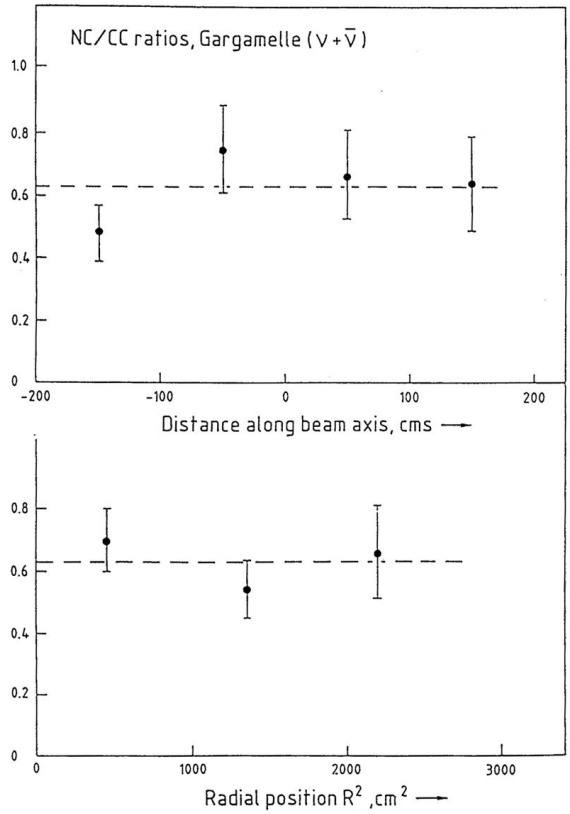

Figure 28 Radial and longitudinal distribution of the relative rate of neutral current candidates in the Gargamelle chamber.

The results were contested during 1973 by the HWPF experiment which had just started at Fermilab and which used a high energy neutrino beam and a calorimeter and magnetic spectrometer apparatus. Because of the underestimation of hadrons penetration in the calorimeter which faked muons, a fraction of NC events were identified as CC by HWPF and after background subtraction no NC events were left.

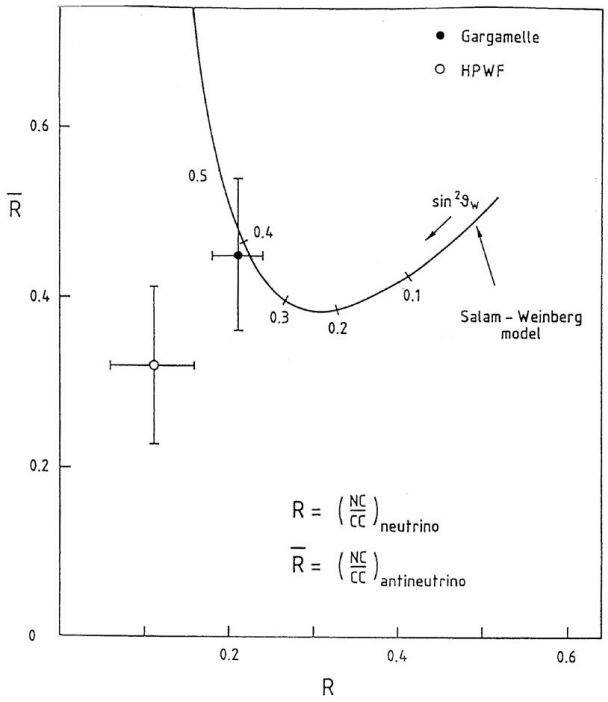

Figure 29 The 1974 Gargamelle and HPWF results on $\sin^2\theta_w$ obtained from neutral current relative rate in ν and $\bar{\nu}$ beams.

However, by the end of 1974, this defect was corrected and the Gargamelle results confirmed.

After this discovery accurate measurements of R were used (1975-2000) to measure $\sin^2\theta_w$ or more precisely the ratio $M_w/M_z = \cos\theta_w$.

$$R_\nu \approx \frac{1}{2}\frac{M_w^4}{M_z^4}\left(1 + f\left(\frac{\nu cc}{\bar{\nu} cc}, sin^2\theta_w\right)\right)$$

$$f \sim .05$$

The f term is only a 5 % correction. Structure function uncertainties cancel almost perfectly in the R ratio except for a small asymmetry caused by the charm quark mass. (In CC interaction strange sea quarks are changed to heavier charm quarks).

This effect was the cause of the main systematic error. As shown in figure 30, the principle of the measurement for high energy neutrino interaction was a separation of the NC and CC events by the event length.

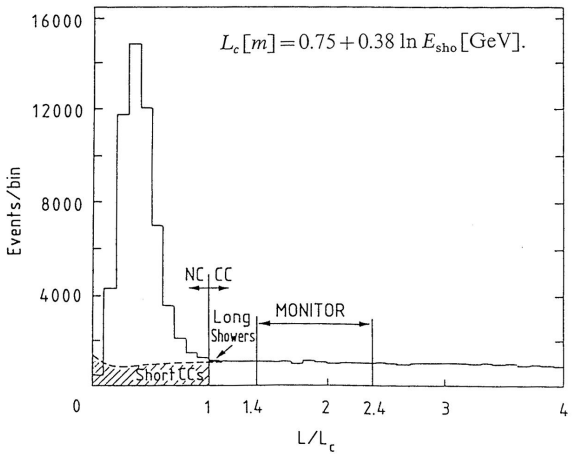

Figure 30 Event length distribution in high energy neutrino experiments. NC events have a short length typical of hadronic shower while, for CC events, the length is dominated by muon penetration.

R was gradually measured to 1% (CDHS and CHARM in 1987-1988) or even better CCFR (1994-1998) the derived $\sin^2\theta_w$ values were 0.231 ± 0.006 and 0.224 ± 0.004 the final error being dominated by systematics.

A breakthrough in accuracy was recently obtained by the NuTeV experiment at Fermilab, it used both ν and $\bar{\nu}$ interactions to depend only on valence quark interaction and therefore suppress the uncertainty of the CC events on the strange sea quarks. This last measurement gave $\sin^2\theta_w = 0.2253 \pm 0.0022$

2.2. DISCOVERY OF THE W AND Z BOSONS

After the neutral current discovery and early measurements of $\sin^2\theta_w$ the W and Z mass could be predicted to be around 80 and 90 GeV respectively, out of reach of any existing accelerator. In hadron-hadron collisions, a centre of mass energy greater than 500 GeV was needed. The first proton-proton collider, the ISR was approved for construction in 1965 and used first in 1971 but its energy was much too low.

In 1977, Cline, McIntire and Rubbia proposed to convert the Fermilab accelerator into a proton antiproton collider. The use of antiproton increased the probability of obtaining high energy quark antiquark collisions and furthermore allowed to store both beam in a single ring, the main problem being to prepare a low emittance intense antiproton beam.

The idea of doing $p\bar{p}$ collisions had been proposed originally by Budker from Novossibirsk at the 1966 Saclay accelerator conference. In the original Fermilab proposal, as in Budker's proposal, the idea was to decrease the emittance of low energy antiprotons (cooling) by collisions with a high intensity, low emittance electron beam having the same velocity.

After the Fermilab proposal was turned down a similar proposal was presented to CERN by Rubbia and approved in 1978 and first collisions observed in 1981 an incredibly short time for such a complicated accelerator and apparatus.

2.2.1 The collider.

The machine breakthrough was the invention around 1968 by S. Van der Meer (who shared with C. Rubbia the Nobel prize for the W,Z discovery) of the principle of stochastic cooling. The principle is shown in figure 31: if a single particle position with respect to the central orbit is sensed and corrected by a kicker after (n/2 + 1/4) betatron wavelength, then clearly this particle can be placed on the central orbit.

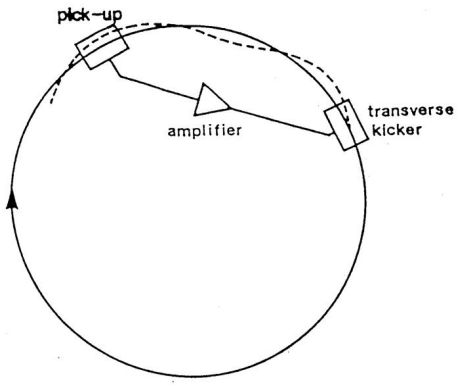

Figure 31 Schematics of the feedback needed for stochastic cooling.

If n particles are sensed, in a short time, by a high frequency system, then the mean orbit can be corrected and the beam size σ is reduced:

$$\sigma_f^2 = \sigma_i^2 - \bar{x}^2$$

Where $\bar{x} = \sigma/\sqrt{n}$ is the average position which is corrected. The cooling continues because the sample composition changes due to the spread in revolution frequency.

Momentum or longitudinal cooling can be performed in a similar way, except that the momentum offset is detected by a shift in orbit frequency which is compensated by acceleration or deccelaration. In practice sophisticated and complicated procedures were used to cool rapidly (every 2 sec) each batch of $10^6\bar{p}$ and cool gradually over 12 hours a full stack of $10^{11}\bar{p}$ (fig. 32 and fig. 33).

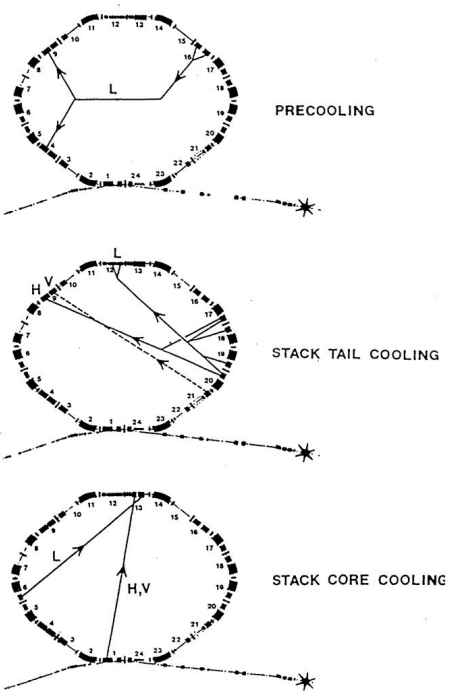

Figure 32 The many cooling systems needed to prepare efficiently a cooled stack of $10^{11}\bar{p}$.

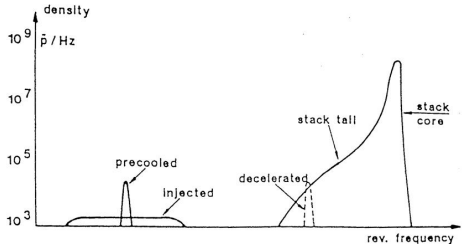

Figure 33 Density in revolution frequency, i.e. in momentum, of the injected $\bar{p}$ and the main stack of antiprotons.

2.2.2 The experimental apparatus .

The UA2 apparatus was described in the preceding chapter, while being ideal for jet observation it was not as good as UA1 for W discovery because of incomplete solid angle, UA1 will be briefly described here.

The key observation was the following: in W$\rightarrow e\nu, \mu\nu$ decays there will be, because of the unobserved ν, 40 GeV of missing momentum in the observed particles. However in q+$\bar{\text{q}}$ $\rightarrow$W the W longitudinal momentum is not known event by event, the useful signature is therefore missing transverse momentum i.e. an apparatus hermetic in azimuth and with a coverage down to small polar angle is needed. UA1 was the first of the

general purpose hadron collider detectors. As can be seen in figure 34, it was a complete apparatus measuring charged particles, gammas, and neutral hadrons and identifying electrons and muons.

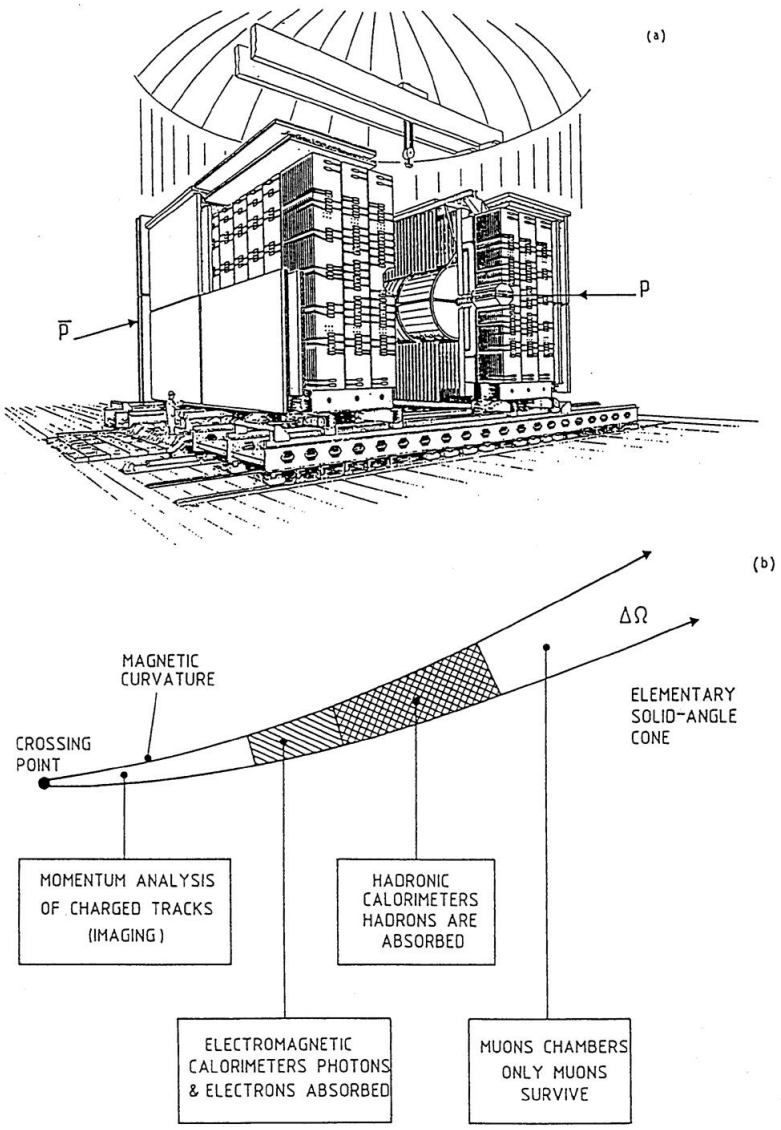

Figure 34 Side view of the UA1 apparatus and description of the role of the successive layers.

For the W discovery, the trigger selected high P_t electrons (muons were used later). The following event samples with electrons $P_t > 15$ GeV were collected:

$$291 \text{ electrons} + \text{jets in a cone} \Delta\phi = 180^\circ \pm 15^\circ$$

$$55 \text{ electrons with no opposed jets}$$

Figure 35 shows with a slightly larger sample the corresponding missing E_t distribution, which peaks at 40 GeV as expected for W production. A transverse mass M_t is calculated from the electron P_t and the missing E_t. With the help of Monte-Carlo correction the W mass is fitted to the M_t distribution a value of 81 ± 1.5 GeV was obtained in 1983.

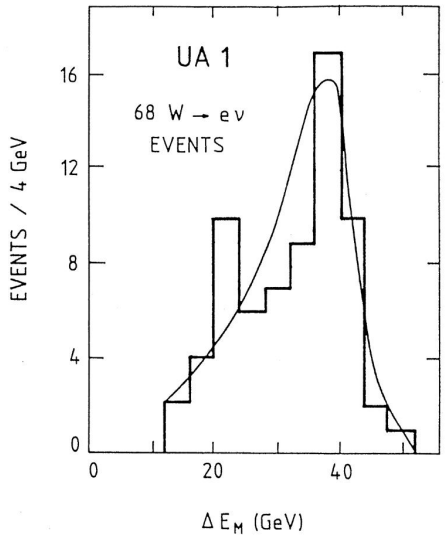

Figure 35 The distribution of missing transverse energy for those events in which there is a single electron with $P_t > 15$ GeV/c and no coplanar jet activity.

The rate of Z production was expected to be ten times smaller, because of the higher mass and of the smaller leptonic branching ratio. On the other hand, the high lepton pair mass allows an almost backgroundless signature. First signals were seen in 1994, using electrons and muon pairs in UA1 and electron pairs in UA2. A clear peak was visible, as shown in figure 36.

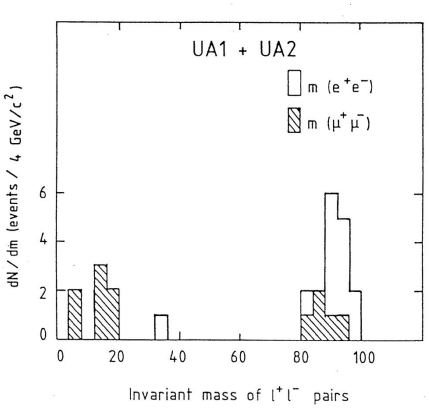

Figure 36 Invariant mass distribution of dilepton events from UA1 and UA2 experiments. A clear Z° peak is seen at a mass of about 95 GeV/c^2.

2.3. A NEW QUARK : CHARM (THE 1974 "NOVEMBER REVOLUTION")

The discovery of the new quark, charm, caused an earthquake-type shock in the community. At first the interpretation was not obvious and then gradually this discovery not only gave enormous confidence to the electroweak standard model but it gave an enormous boost to the idea that quarks were "real". This was based on the partly naive idea that with the discovery of a heavy quark one would obtain the equivalent to the hydrogen atom for quark physics. Retrospectively one could say that theorist had been calling for such an object, but this was not generally realized. The GIM mechanism (discovered in 1969-1970) used a fourth quark to cancel $\Delta S=1$ neutral currents for example in box diagrams (fig. 37). The cancellation is up to terms

$$(m_c^2 - m_u^2)/m_{\mathrm{w}}^2$$

From this the mass of the new charm quarks was predicted to be less than a few GeV. By the summer of 1974 a phenomenological article by M.K. Gaillard, B. Lee and J.L. Rosner gave recipes for charm search with detailed predictions of a narrow $c\bar{c}$ state decaying to $\mu^+\mu^-$ and e^+e^-, however these predictions were not the direct cause of the searches at Brookhaven and SLAC. The apparatus used at Brookhaven for the J discovery by S. Ting et al., was a major change compared to the previous Lederman apparatus looking at muon pairs, the main emphasis was on mass resolution and identification redundancy.

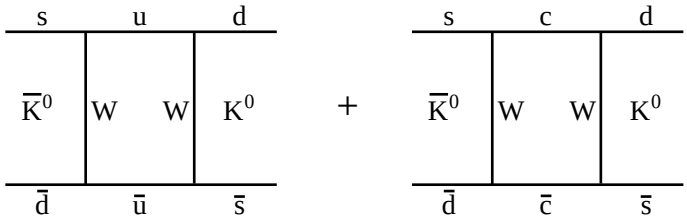

Figure 37 Box diagrams responsible for K_0 $\bar{K_0}$ oscillation. The amplitude from the two diagrams have opposite signs and cancel each other

To obtain a good angular resolution the massive hadron absorber which caused multiple scattering in the muon experiment had to be abandoned. Because of the huge background from hadron decays to muon, it was then decided to detect electron pairs instead of muons. A powerful 2 arm magnetic spectrometer was used to measure the electrons angle and momentum and the hadron background was rejected by a redundant set of Cerenkov counters and shower counters (Fig. 38).

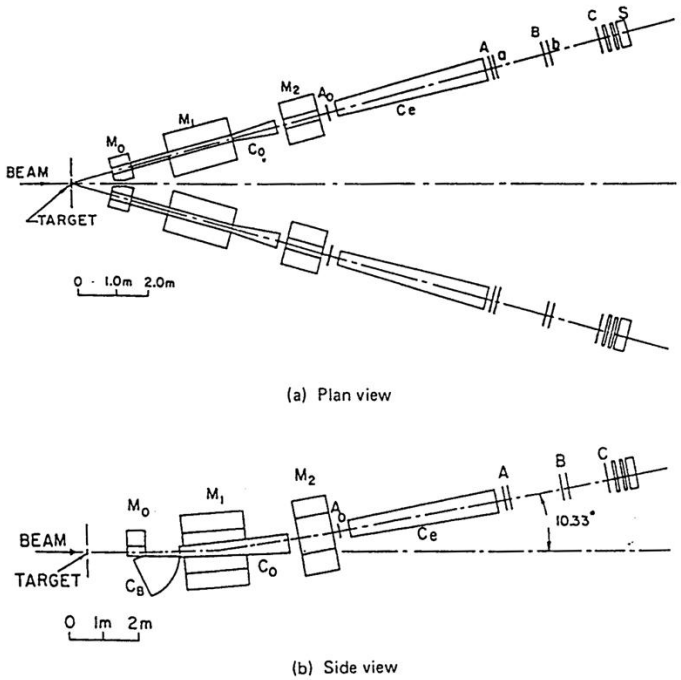

Figure 38 Plan and side view of the spectrometer used by the group of S. Ting et al. for the J discovery.

The spectrometer mass resolution was about 20 MeV a 0.6% mass resolution compared to the 16, 20 % mass resolution of the previous BNL experiment.

The mass distribution obtained is shown in figure 39 together with the result of the previous experiment which was optimised for high counting rate instead of resolution.

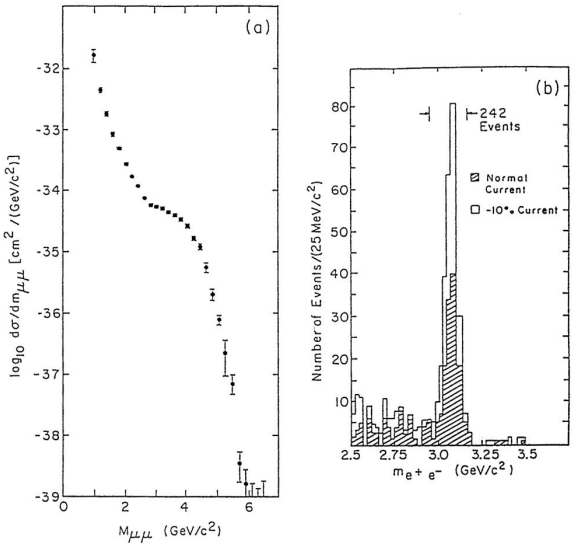

Figure 39 Dilepton mass distributions, a) in the BNL Lederman et al., experiment and b) in the S. Ting et al. experiment.

As everybody knows the $c\bar{c}$ state was discovered simultaneously at SLAC (and called the ψ). The 3-6 GeV e^+e^- colliding ring called SPEAR was probably the accelerator with the greatest number of first class discoveries in the history of our science. (Some were already mentioned in the previous chapter).

These discoveries were sometime simply due to the good choice of energy but the design of the apparatus (MARKI) played an important role in the open charm and τ discoveries. The MARKI detector (fig. 40), built in 1973, can be seen as a prototype of many future e^+e^- collider detectors.

It had the following main strong points: It had a full and homogeneous ϕ acceptance and a good if not excellent $\cos\theta$ acceptance, it was a complete detector with charge particle tracking, gamma detection, electron and muon identification and some K,π separation using time of flight.

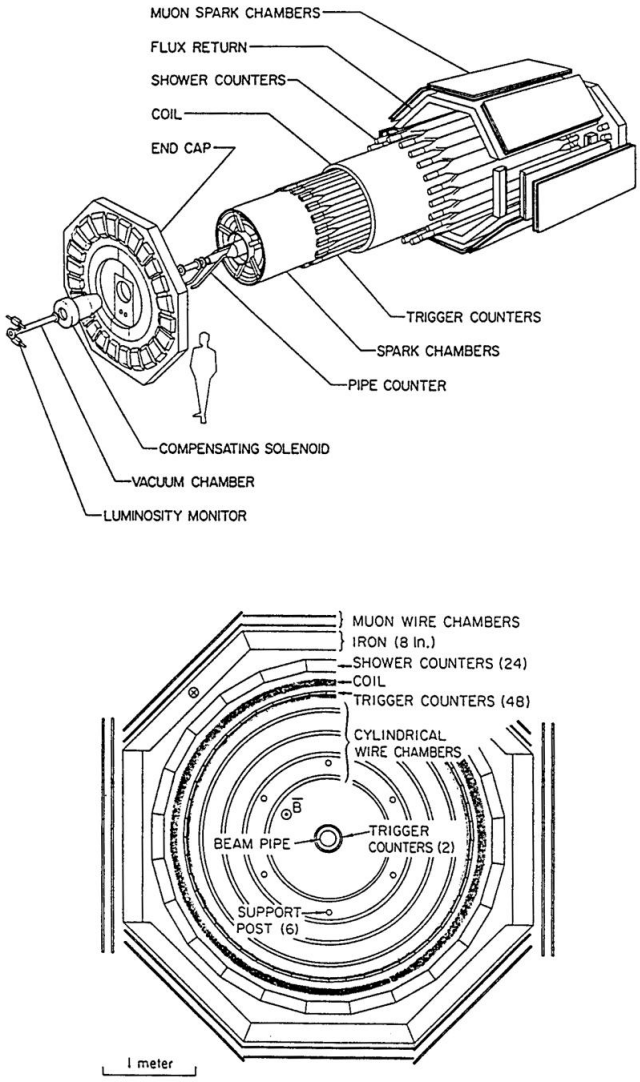

Figure 40 Views of the MARKI apparatus showing the detector layers.

The construction was done by a collaboration which resulted from a remarkable marriage of SLAC apparatus experts and Berkeley software experts (coming from the bubble chamber groups).

The ψ was discovered by a scan of the machine energy. The resonance was initially seen because collision cross-section above the resonance is

also increased due to the emission of bremshtrahlung photons by the colliding e^+e^-. When the peak cross-section was found, the increase above the non resonant region was incredibly high (a factor of more than 100 !).

Initially there was much confusion on the interpretation of the discovery and various hypothesis explored (I remember an explanation which identified the 3 GeV object with the Z° boson !).

However a few months later, detailed results on production of hadrons muons and Bhabha events were produced (fig. 41).

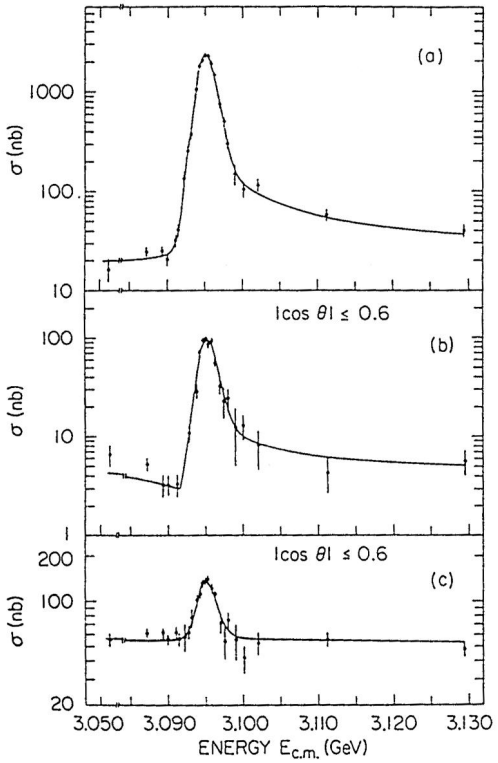

Figure 41 The ψ resonnance cross-section as function of center of mass energy in a) the hadronic charmed, b) the muon channel and c) the Bhabha channel.

From these results the branching ratios and total width of the J/ψ could be derived (Table 1), from these it was clear that, even if very narrow, the resonance was too wide to be due to a pure electromagnetic coupling (the γh branching ratio 12 KeV is narrower than the total width) and the "hidden charm" hypothesis was accepted.

Table 1 Properties of $\psi(3095)$

Mass	3095 ± 0.0004 GeV
J^{PC}	1 - -
Γ_e	4.8± 0.06 KeV
Γ_μ	4.8± 0.06 KeV
Γ_h	59± 14 KeV
$\Gamma_{\gamma h}$	12± 2 KeV
Γ	69± 15 KeV
Γ_e/Γ	0.069± 0.009
Γ_μ/Γ	0.069± 0.009
Γ_h/Γ	0.86± 0.02
Γ_μ/Γ_e	1.00± 0.05

However no charm mesons were seen before 1976. Because of combinatorial background it was very difficult to see the D$\rightarrow K\pi$ decay; the breakthrough came from the use of K identification using time of flight. The separation was marginal (on average 0.5 ns with a resolution of 0.5 ns) but weighting each event with its K identification probability improved sufficiently the signal to noise ratio.

2.4. THE THIRD FAMILY: THE τ LEPTON AND B QUARK

Contrary to neutral current or charm discovery there was no strong advice from theorists on the existence of a third family (it must be admitted that charm was anyhow discovered independently of these advices). Koyabashi and Maskawa had proposed in 1973 that the existence of a third quark family could explain CP violation in K decay by a phase in a 3 family CKM matrix, but searches of a third lepton heavier than muon or electron had been proposed much earlier (around 1970).

2.4.1 τ discovery.

The τ was discovered, in 1975, on the MARKI apparatus at SLAC by M. Perl et al. The key idea of the analysis was that, in analogy to $\mu \rightarrow e\nu\bar{\nu}$ decay, one expect the τ to decay both to $e\nu\bar{\nu}$ and to $\mu\nu\bar{\nu}$. Then in the reaction $e^+e^- \rightarrow \tau^+\tau^-$ it is expected that some events will be seen as acollinear eμ particles accompanied by missing momentum.

The big experimental problem of the experiment was the limited quality of the lepton identification: The μ's were identified by penetration in the iron used for magnetic flux return which was only 1.7 interac-

tion length thick. The electrons were signed by characteristic pulses in shower counters which were however of rather poor quality; because of this, hadron misidentification probability was about 20% instead of the 1% or better now achieved in modern apparatus. The 1975 results are shown in table 2. The number of $e\mu$ events, when compared to the numbers of eh and μh events, could not be explained by hadron misidentification. There was therefore, in the article, the claim of a new phenomenon and the existence of a new lepton was presented carefully as a possible explanation. By 1977 the apparatus had been improved, τ decays to hadrons could be observed in eh events and the τ existence was generally accepted.

Table 2 Table of acollinear ($\Delta\theta > 20°$) events used in τ lepton discovery. All particles momenta are greater than 0.65 GeV/c.

	Total Charge = 0			Total Charge = $\pm$ 2		
Number Photons =	0	1	> 1	0	1	> 1
ee	40	111	55	0	1	0
eμ	24	8	8	0	0	3
μμ	16	15	6	0	0	0
eh	18	23	32	2	3	3
μh	15	16	31	4	0	5
hh	13	11	30	10	4	6
Sum	126	184	162	16	8	17

2.4.2 b quark discovery.

Actually, as in the case of charm, the first sign of this new quark was seen in the form of a hidden beauty $b\bar{b}$ state, the Υ, seen in its decay mode to lepton pairs (e^+e^- or $\mu^+\mu^-$). The discovery was done in 1976-1977 at Fermilab by the group of Lederman et al. It was clear by then that the secret of the discovery of narrow states was to obtain an excellent mass resolution, and, in its first attempt, the group chose to observe e^+e^- pairs, as had been done at BNL by the group of Ting et al. for the J discovery. This first run was done in 1976 in a two arm spectrometer, a mass resolution of < 70 MeV was obtained,

but, because of the open configuration of the spectrometer needed to observe electrons, the interaction rate in the target had to be limited to 5×10^9 interactions/accelerator spill. This was marginal to observe, with enough rate, a high mass resonance produced with a small cross-section. The group then switched back, in 1977, to a dimuon configuration but the breakthrough compared to the BNL dimuon experiment was to absorb the hadrons with 7 meters of Beryllium rather than with iron. This improved the radiation length to interaction length ratio by a factor 8 and consequently the angular error contribution to the mass resolution. The muons momenta were measured by powerful air-core magnet spectrometers and muon identification was checked by further absorber and momentum remeasurements in iron core magnets. A mass resolution of 200 MeV was obtained.
The apparatus is shown on figure 42. As can be seen in figure 43 a triple structure was seen corresponding to the three 1^- states $\Upsilon, \Upsilon', \Upsilon''$.

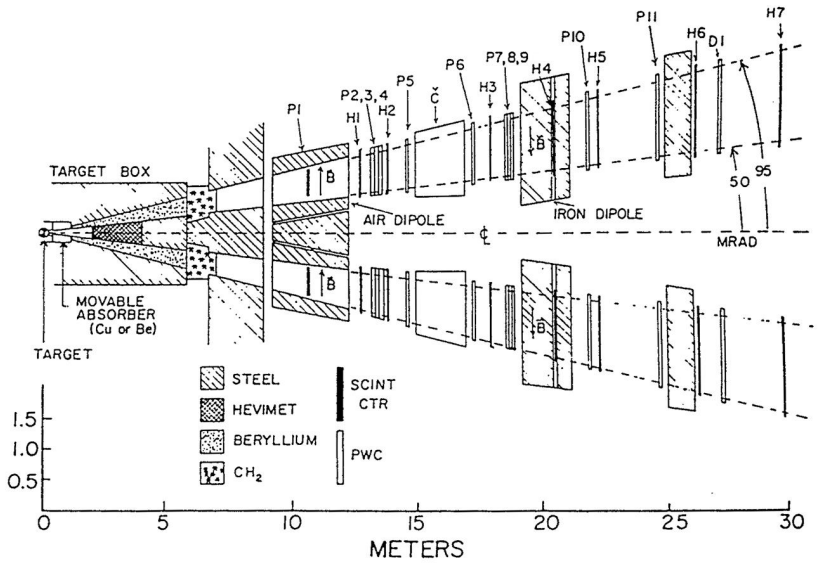

Figure 42 The dimuon spectrometer used by the group of Lederman et al. at Fermilab for the Υ discovery.

Soon after, the Υs were next observed by the DASP, PLUTO, and DESY HEIDELBERG experiments at the Doris e^+e^- collider which could be pushed to the necessary energy. The peak of the Υ and Υ' were clearly observed. As with the J/ψ when the cross-section and leptonic branching ratio were measured the leptonic partial width could be determined.

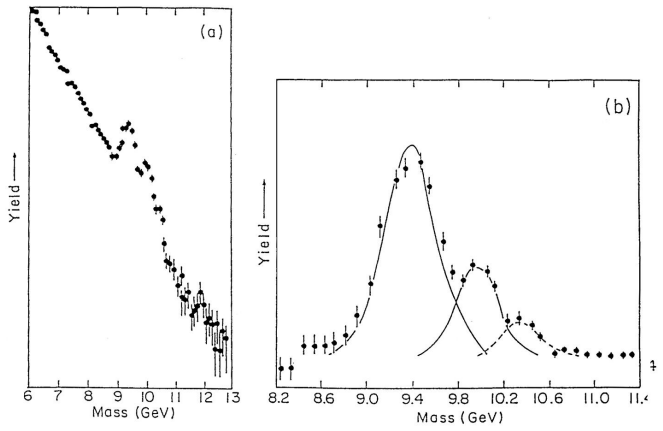

Figure 43 The dimuon mass spectrum a) observed in the experiment of Lederman et al. The spectrum after Drell-Yan background and subtraction is shown in b).

A value of $\Gamma ee = 1.3$ KeV was found while the equivalent value for the J/ψ was 5.4 KeV. This indicated that the b quark had a 1/3 charge (compared to the 2/3 value for the c-quark). As it was the case for charm the discovery of the B meson was much more difficult and it was only 7 years later that the Argus experiment at Doris (DESY) and the Cleo experiment at CESR (Cornell) showed evidence for the decay B$\rightarrow D$ or $D^* + \pi$.

The last quark, the top was found at Fermilab in 1994 but this is a recent story, which the attendants of this school have certainly heard on many occasions.

3. LEP AND SLC THE IDEAL MACHINES FOR STANDARD MODEL STUDIES

The data from LEP and SLC allowed to test the standard model with an unprecedented accuracy, an accuracy which even surpassed by factors of 3 to 4 the best expectations listed in the various workshops preparing, in the 80's, the physics before the start of the colliders. These accurate tests, as is well known, not only reinforced strongly our belief that we were using the correct theoretical framework, but also allowed to predict points of the models (for example the Higgs mass) which could be out of present experimental reach. Since these LEP, SLC results are fairly recent and many reviews exist on this physics, in summer schools and conferences, I will be quite brief, in the written version, on results presentation.

3.1. THE DETECTORS

However I think worthwhile to try to explain how this remarkable progress in accuracy was obtained. It should be remembered that the typical level of accuracy of previous e^+e^- experiments was about 5-10 %, while the accuracy obtained at LEP/SLC is of order 0.1 % to 0.5 % ! I will give a somewhat biased account by concentrating on the ALEPH apparatus to which I have contributed; however similar accuracies were obtained by DELPHI L3 OPAL and SLD and therefore, in some way, my explanations apply to all five apparatus.

- Starting with the most obvious fact, the large number of events helped. Each LEPI experiment collected about 4 millions Z°, and the large statistics allowed also better tests of systematical errors. However millions of J/ψ events were collected in previous machines without comparable accuracy improvement, so large statistics is not the full answer.

- High energy helped also: Calorimeters work better at high energy, and hard to see low momentum particles play a much smaller role; finally a large fraction of Z° physics is obtained in events with two back to back jets. These events allowed powerful test of the apparatus, or model, systematics by tagging one hemisphere and studying the efficiency of jets or particles in the opposite hemisphere.

There was also an evolution to a much better apparatus. The key breakthrough, in my opinion, was the emphasis on small inefficiencies and on redundancy: If α is the fraction of events selected or measured in a redundant way and $(1-\epsilon)$ is the inefficiency of the apparatus for these selection or measurements, then it can be derived that the lost event fraction $(1-\epsilon)$ can be determined with a relative statistical error of $\sqrt{(1-\epsilon)/N\alpha)}$ (N being the number of events). If $(1-\epsilon)$ is small and α large, then the systematical error from the acceptance is determined by the data and small compared to the overall statistical error. In order to implement those constraints on ϵ and α, the emphasis in ALEPH was put on an hermetic apparatus (figure 44).

A small granularity was required in order to keep high efficiency for narrow jet events or high energy τ lepton decays. The track detectors consist of 2 layers of silicon strip detectors (each with r-ϕ and Z readout) followed by an 8 layer wire chamber (the ITC) and by a TPC. The TPC gave 21 space point measurements for each track, DE/DX was measured in TPC wires but also on the space points (though with a reduced accuracy).

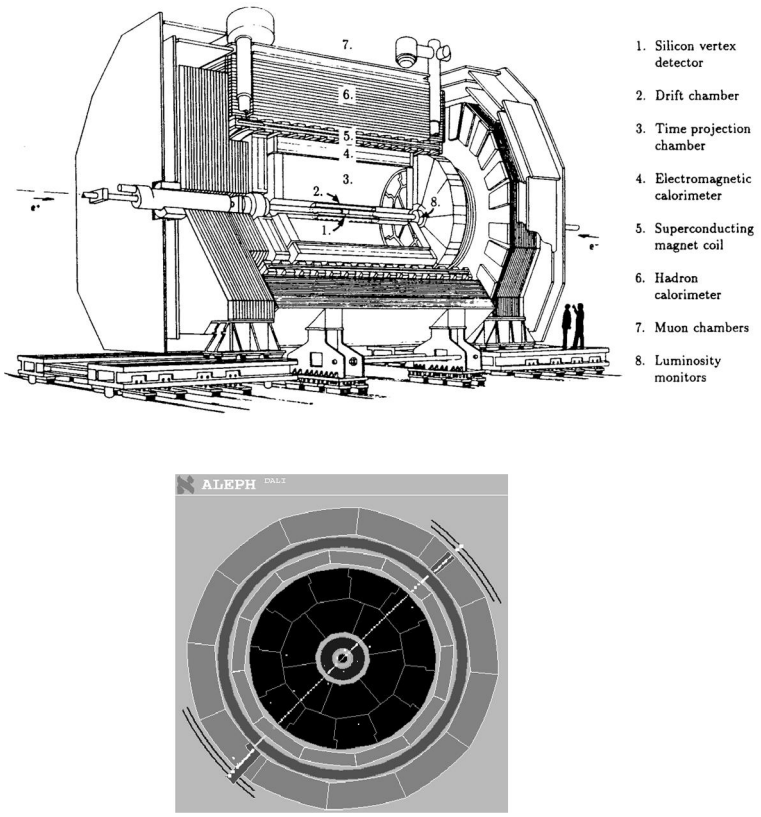

Figure 44 Perspective view of the Aleph apparatus and r-ϕ view of a $\mu\mu$ event display.

Because of the overlapping sector structure, there was no single track inefficiency at large angle ($|\cos\theta| < 0.8$). At smaller angle a small 1.5 % inefficiency, modulated in ϕ, was due to sector edge effect; it was calibrated to 0.03 % accuracy with redundant events. In the large angle region the track inefficiency in dense $q\bar{q}$ jet events was only 0.3 %.

The calorimeter measurements exploited also granularity and redundancy, there was a full overlap between the barrel and encap elements and, in this overlap, resolution was worsened (and calibrated) but efficiency was maintained. Holes of 3 to 5 % exist in ϕ between the calorimeter modules but holes in ECAL and HCAL were not aligned preserving efficiency for photons over all the solid angle. Both calorimeters were made of sandwiches of wire chambers and passive material (lead for ECAL, iron for HCAL).

In both cases, there was a redundant readout system: the signals were read both from the wire planes or wire strip and on cathode pads forming towers. Rare events with malfunctioning of one of the readouts were thus easily detected in the data. The muon identification was also redundant and done either by penetration through the layers of HCAL or by signals observed in two layers of muon chambers placed behind HCAL. In jets, muon efficiency of 86 % was reached with typical hadron misidentification of 0.8 %. The electron identification was done independently, either by shower energy and shape in ECAL or by DE/DX measurement in the TPC. In jets, a typical electron efficiency of 65 % was reached with hadron misidentification of 0.1 %. In cleaner environment, like τ decays better performance were obtained (table 3).

Table 3

Tau decays $\rightarrow$ identified as $\downarrow$	$e\nu\nu$	$\mu\nu\nu$	$h + n\pi^0\nu$
electron	0.995	0.000	0.006
muon	0.000	0.992	0.010
hadron	0.005	0.008	0.984

All the above efficiencies and misidentification were obtained from the data, exploiting the redundancy of the apparatus. When compared for example with the MARKI τ discovery results (table 2) one can see the identification improvement of 20-30 typical of the LEP/SLC era.

The trigger was done mostly on the existence of at least one energetic track or jet in one hemisphere, the other hemisphere offering a redundant confirmation and check. Trigger inefficiencies were therefore minute (less than 10^{-4} !).

Finally, the luminosity was measured by Bhabha events in small angle calorimeters. After an initial stage, all experiments adopted the use of high accuracy tungsten-silicon pad calorimeters which reached shower position accuracy of about 10 microns. The experimental luminosity error was thus about 0.07 % and, with the remarkable progress, obtained by the group of Jadach et al., on the evaluation of high order radiative corrections, the theoretical small angle Bhabha cross-section was known with similar accuracy. Finally the Z hadronic cross-section was evaluated with a 0.1 % accuracy, a progress of almost 2 orders of magnitude compared to statistical or systematical errors reached in previous experiments.

3.2. ELECTROWEAK RESULTS

The most important result obtained from the initial data of SLC and LEP was to establish the number of neutrino families.

From a measurement of the Z° cross-section as function of energy, it is possible to extract the total width of the Z°. If the hadronic (Γ_h) and leptonic (Γ_e Γ_μ Γ_τ) are taken from theory then the invisible width can be derived $\Gamma_{inv} = \Gamma_z - \Gamma_h - \Gamma_e - \Gamma_\mu - \Gamma_\tau$ and the number of neutrino family obtained from $N_\nu = \Gamma_{inv}/\Gamma_\nu$. However, in the years of preparation of the MARKII experiment at SLC, G. Feldman remarked that this method had a rather large statistical error for a given total integrated luminosity. He suggested instead to obtain the Z° total width from the peak hadronic cross-section.

$$\sigma_h = (12\pi\Gamma_e\Gamma_h)/M_z^2\Gamma_z^2)$$

This method because of its improved accuracy was used by all experiments for obtaining the initial value of N_ν.

In the summer of 89 MARKII at SLC obtained its first result N_ν =2.7 ± 0.7. By the end of 89, after the start of LEP in September the result from the average of ALEPH, DELPHI, L3 and OPAL was N_ν = 2.99 ± 0.13. This was a key measurement since, at that time, there was no compelling arguments (other than cosmological) against the existence of a fourth family of heavy quarks and leptons; within the usual assumption of small neutrino masses the 1989 results fixed the number of family to three. The most recent result on Nν is Nν = 2.9835 ± 0.008, this can be interpreted as a limit on unexpected decay mode of the Z° to invisible particles $\Delta\Gamma_{inv} < 2$ MeV, i.e. $\Delta\Gamma_{inv}/\Gamma_z < 0.08\%$.

The next important step in precise electroweak measurement was to obtain informations, on higher order electroweak corrections. Examples of such corrections induced by top quark loops are given in figure 45.

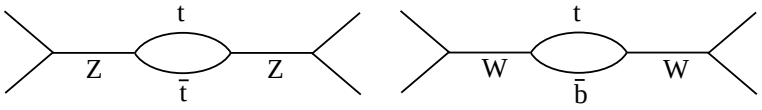

Figure 45 Top loop diagrams responsible for radiative corrections to W and Z° masses and couplings.

From measurements of G_μ, the Z° mass, and width and couplings measured from Z pole asymetries, the top quark mass could be predicted. Initially most of the accuracy came from the LEP data but later with

the use of a polarized electron beam at the SLC, SLD contributed also very significantly to the evaluation of electroweak corrections.

Already the first 1989 LEP results predicted the top mass to be large (180 GeV ± 60 GeV). By the 1993 summer conference the prediction was refined to $M_{top} = 162 \pm 16$ GeV ± 20 GeV as shown on figure 46, the last error represents the uncertainty on another correction due to a Higgs boson loop, and the range of the uncertainty corresponded at the time to a range of possible values for the Higgs mass of 60 GeV to 1000 GeV.

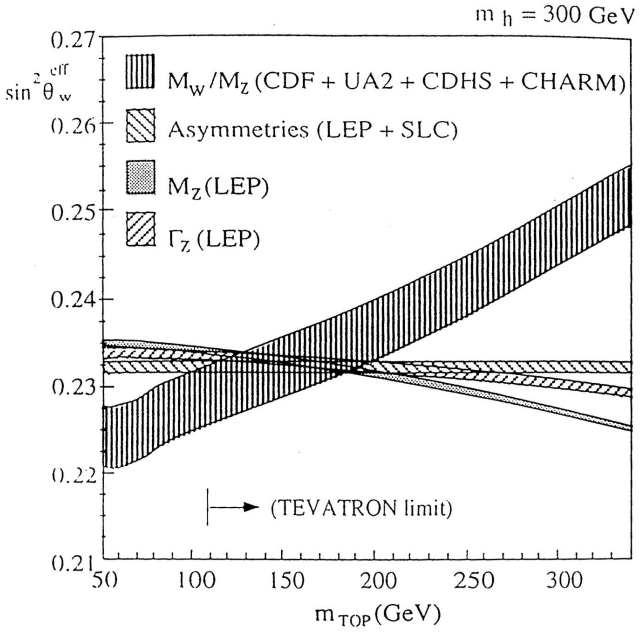

Figure 46 Calculated $\sin^2\theta_w$ values as function of M_{top} for four different experimental inputs. The intersect defines the predicted value of M_{top}.

Soon after, in 1994, the top quark discovery was announced at the Fermilab $p\bar{p}$ collider and its mass measured to be in agreement with the prediction. The most recent M_{top} measurement is $M_{top} = 174.3 \pm 5.1$ GeV and the most accurate prediction from an overall fit of all other electroweak observable, including W mass measurements at LEPII and $p\bar{p}$ colliders is $M_{top} = 167\ ^{+11}_{-8}$ GeV a stunning success for the standard model consistency. Actually inserting into the fit the experimental M_{top} value, it is possible to obtain a bound on the

mass of the standard model Higgs mass, the value is predicted to be less than 215 GeV at 95 % confidence level.

LEP and SLC have also contributed important and accurate results in the field of B physics and QCD but a complete review would be outside the scope of these lectures.

4. CONCLUSION

Establishing beyond doubts the main features of the standard model has been a long process.

Clearly this process was often guided by remarkable theorist insights, but decisive experimental discoveries had a key role. Progress has been more slow, difficult, and painful than it is remembered by our forgiving memory.

The main ingredient of the model the Higgs' boson is still missing and signs of effect beyond the standard model have been recently seen in ν oscillation, so the coming 2000-2010 period promises to be very interesting.